

An Experimental Study of Bubble Motion on a Heating Surface in Nucleate Boiling

By

Itaru MICHİYOSHI* and Tsuyoshi NAKAJIMA*

(Received June 23, 1964)

This paper deals with some results of the observations of bubble formation and growth in nucleate boiling on a horizontal heating surface immersed in water under atmospheric pressure by using a high-speed camera. Experimental data are compared with Zuber's or Griffith's analytical results for the prediction of bubble growth rate. Some discussions are also presented for the preparing period and the growing period of one cycle of bubbling.

1. Introduction

Although all bubbles can not be treated as an isolated bubble in nucleate boiling, it is sure that the bubble motion is an important factor to characterize nucleate boiling heat transfer.

As described in the previous paper¹⁾, the bubbles are periodically regenerated on the heating surface, as the circumstance, in which nucleation can occur and the formation of new bubble can proceed, is periodically reestablished after the bubbles are detached from the surface. Therefore, one cycle of bubbling can be considered by a model as shown in Fig. 1.

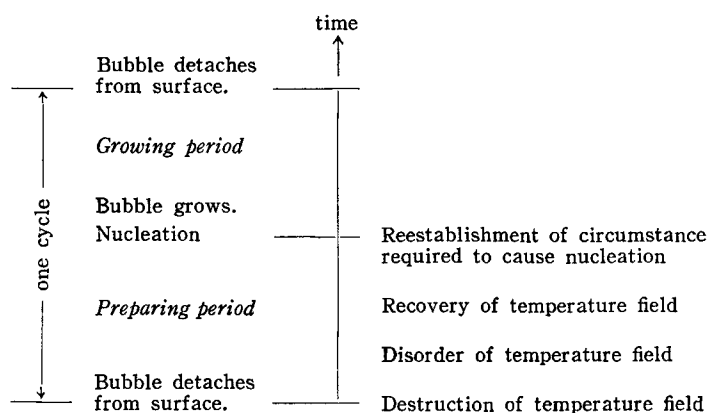


Fig. 1. One cycle of bubbling.

* Department of Nuclear Engineering

The experiments were performed to investigate the bubble formation and growth. A theoretical analysis of preparing period which is derived by considering transient heat conduction is compared with experimental data. Zuber's or Griffith's theory for the prediction of bubble growth rate is discussed. Some discussion will be also given to the relationship between diameter of detached bubble and frequency of bubbling.

2. Apparatus and Procedure

The pool boiling apparatus are shown schematically in Fig. 2. A high-speed camera capable of film speeds up to 10,000 frames per second was employed in the photography. The heating specimen was a stainless steel ribbon (3 mm width \times 100 mm length \times 50 μ m thickness), which was immersed horizontally in

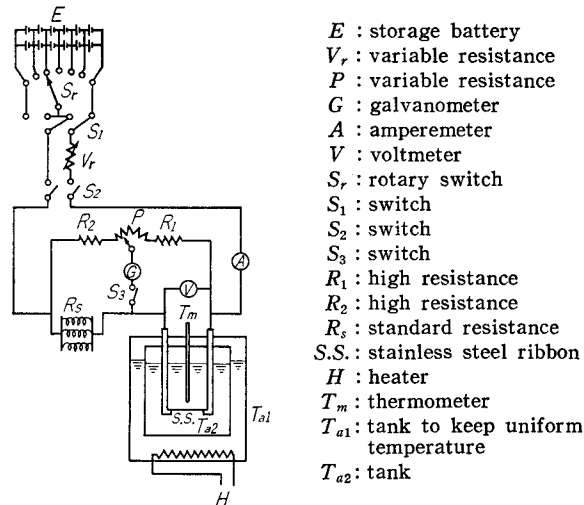


Fig. 2. Pool boiling apparatus.

water and heated electrically; consequently, the heat was transferred from the upper and lower surfaces of ribbon. A thermometer was used to record the water bulk temperature. Wheatstone's bridge was also used to measure the ribbon temperature. By adjusting the electrical power to the ribbon, the bubble population could be controlled. The heating ribbon was not exchanged throughout the present experiment. The bulk temperature was kept to be 97.5°C at atmospheric pressure.

3. Preparing Period

After the bubble detached from the surface, the bubbling elapses until

the nucleation occurs. This is due to the destruction and disorder of the temperature field near the surface caused by the detached bubble. Thus, the preparing period is defined as the time period between the departure of one bubble from the surface and the first appearance of the next bubble. To determine the length of this time period, it is necessary to know: (1) the temperature profile near the surface as a function of time and (2) criteria for the critical temperature profile needed for the bubble nucleus to begin growth. If these two parts are known, it is possible to find the preparing period. If there were no eddy diffusion due to bubble agitation, it would be essentially the case of heat conduction in an infinite slab. Thus, the problem is approximated by the case of one-dimensional transient conduction of heat in a slab.

The one-dimensional heat conduction equation is

$$\frac{\partial T}{\partial t} = \alpha \left(\frac{\partial^2 T}{\partial x^2} \right) \tag{1}$$

with initial condition

$$t = 0; T = f(x) \tag{2}$$

and boundary conditions

$$t > 0, x = 0; T = T_w \quad (\text{constant}) \tag{3}$$

or

$$t > 0, x = 0; -\lambda \left(\frac{\partial T}{\partial x} \right)_{x=0} = q \quad (\text{constant}) \tag{4}$$

Equation (3) means that the heat is transferred from the surface at constant temperature T_w , and Equation (4) the heat is transferred from the surface at constant rate q .

However, it is difficult to give a function $f(x)$. For simplicity, it is assumed that the initial temperature of liquid is uniform temperature T_i at anywhere, i.e.,

$$f(x) = T_i \quad (\text{uniform}) \tag{5}$$

The solution of the differential equation (1) with help of equations (3) and (5) gives

$$T - T_i = (T_w - T_i) \operatorname{erfc} \frac{x}{2\sqrt{\alpha t}} \tag{6}$$

$$\left(\frac{\partial T}{\partial x} \right)_{x=0} = -\frac{T_w - T_i}{\sqrt{\pi \alpha t}} \tag{7}$$

If the actual temperature distribution near the wall is assumed to be a straight line distribution, the slope of this straight line is determined by equation (7). Therefore, the temperature distribution near the wall may be

given by

$$\begin{aligned} T &= T_w + \left(\frac{\partial T}{\partial x} \right)_{x=0} x \\ &= T_w - \frac{T_w - T_i}{\sqrt{\pi \alpha t}} x \end{aligned} \quad (8)$$

In another case the solution of the differential equation (1) with help of equations (4) and (5) gives

$$T = \frac{q}{\lambda} \left[2\sqrt{\frac{\alpha t}{\pi}} e^{-x^2/4\alpha t} - x \operatorname{erfc} \frac{x}{2\sqrt{\alpha t}} \right] + T_i \quad (9)$$

Thus, the temperature of the wall surface T_w increases with time according to the following equation

$$T_w = \frac{2q}{\lambda} \sqrt{\frac{\alpha t}{\pi}} + T_i \quad (10)$$

If the temperature distribution near the wall is assumed to be a straight line distribution in steady state nucleate boiling, in which the heat flux q_0 and the wall temperature T_0 are constant in time, the temperature distribution near the wall may be given by

$$T = T_0 - \frac{q_0}{\lambda} x \quad (11)$$

Using this temperature distribution, Michiyoshi and others¹⁾ calculated the heat energy E expressed by the following equation (12) or (13) and found that the correlation between the heat flux q_0 and the most likely overheating of wall temperature, $T_0 - T_s$, which corresponds to the maximum value of heat energy E_{\max} at given heat flux q_0 , characterizes nucleate boiling heat transfer.

$$E = \int_0^{r^*} \rho_l c (T - T_s) dx \quad (12)$$

or

$$E = \int_0^{2r^*} \rho_l c (T - T_s) dx \quad (13)$$

where r^* is a critical radius of the embryonic bubble given by

$$r^* = \frac{2\sigma}{p_0 \left[\exp \left\{ \frac{A(T_0 - T_s)}{kT_0 T_s} \right\} - 1 \right]} \quad (14)$$

Consequently, if it is assumed that bubble nucleus does not grow until the temperature distribution has become the one given by equation (11), the time required to cause nucleation is derived from equation (8) or (9), respectively, as follows:

$$t_p = \frac{\rho_l c \lambda}{\pi} \left(\frac{T_0 - T_i}{q_0} \right)^2 \quad (\text{for the constant wall temperature}) \quad (15)$$

$$t_p = \frac{\pi}{4} \rho_l c \lambda \left(\frac{T_0 - T_i}{q_0} \right)^2 \quad (\text{for the constant heat flux}) \quad (16)$$

By using equation (13), the wall temperature T_0 corresponding to the maximum heat energy E_{\max} was obtained as a function of $q_0^{1)}$. We took the initial temperature T_i being equal to T_s or T_l . The bulk water temperature T_l was taken as 97.5°C at which the experiments were performed. Fig. 3 illustrates the time interval t_p thus evaluated by solid lines. As shown in this figure, the experimental data for the length of the preparing period varies quite randomly even if the heat flux is constant. As the results of analysis are compared with the experimental results, the agreement of values predicted by equation (15) or (16) with the experimental data is not satisfactory. However, both the theoretical predictions and the experimental data indicate that the preparing period t_p (or the time required to cause nucleation) decreases as heat flux q_0 increases. In order to obtain a good agreement with experimental data, it will be necessary to investigate the effect of disturbance of the thermal layer near the wall which is caused by a detached bubble and its neighboring bubbles. In addition, the further experiments are needed, because the bubble formation in nucleate boiling should be considered statistically.

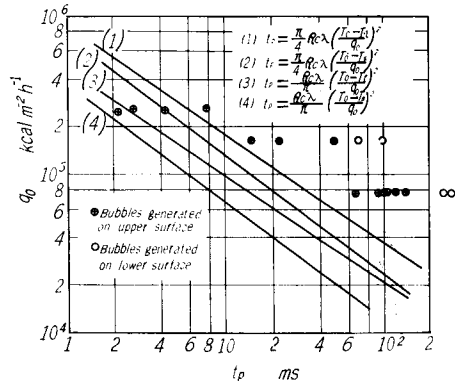


Fig. 3. Preparing period.

4. Bubble Growth Rate

Typical high-speed motion pictures and experimental values of bubble growth are shown in Figs. 4A and 4B. These data were concerned with the bubbles coming from different surfaces of heating specimen: one is the upper surface and the other is the lower surface. The observations of bubble growth were performed under the heat flux q_0 of 7.75×10^4 , 1.62×10^5 and 2.60×10^5 kcal $\text{m}^{-2}\text{h}^{-1}$. In Fig. 4B, bubble diameter D is defined as the diameter of sphere equivalent to the volume of actual bubble.

(1) Effect of positions. Generally speaking, in any cases, after a bubble had grown to a certain extent, the bubble diameter parallel with the wall

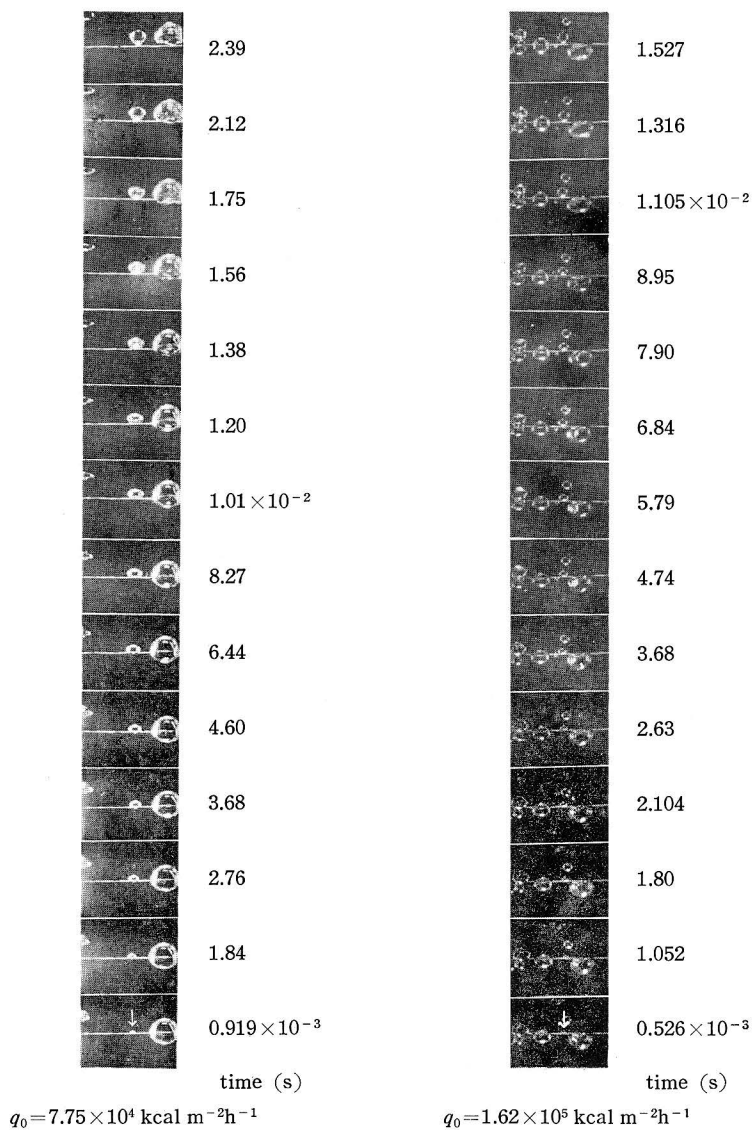


Fig. 4 A. High-speed motion pictures.

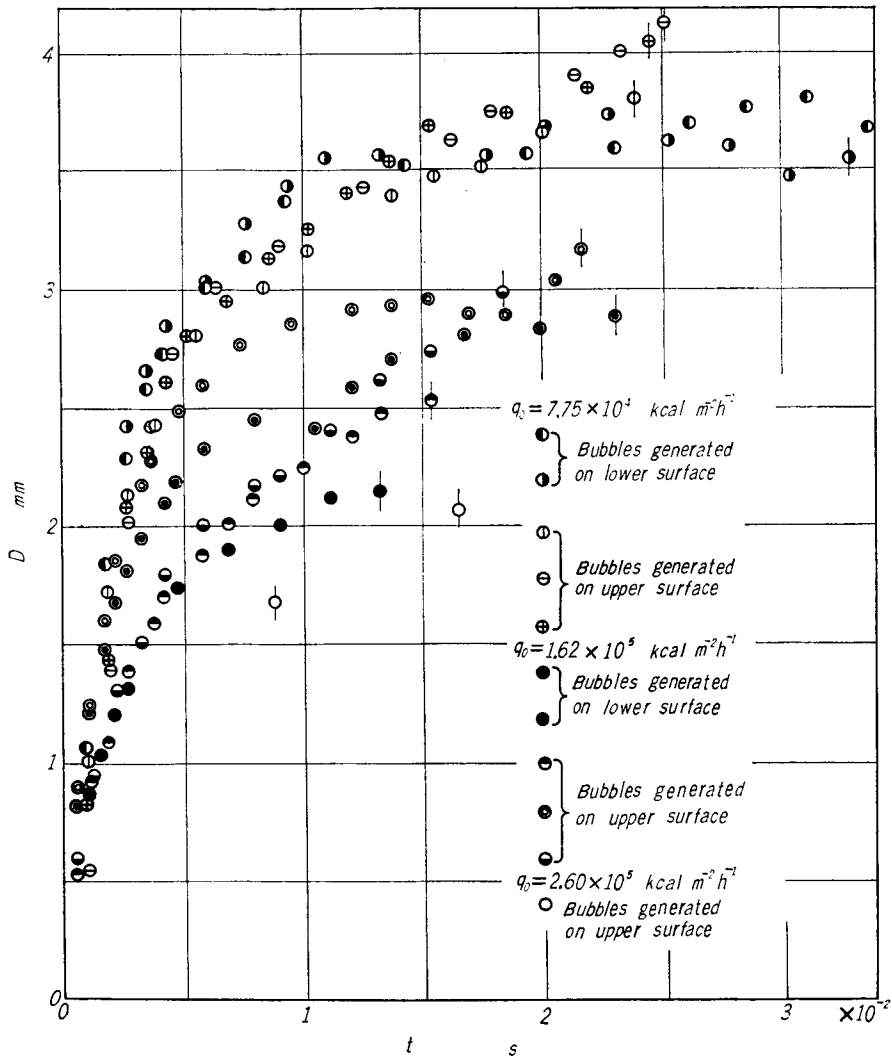


Fig. 4B. Bubble growth rates.

surface was almost constant in time, but the bubble height from the surface still increased. Therefore, the equivalent diameter D was taken as a characteristic length to understand the bubble growth as shown in Fig. 4B. From this figure, there is not much difference in bubble growth occurring on the upper and lower surfaces at given heat flux, from considerations of the statistical scattering of the growth-rate curve. However, when the bubbles detached from the lower surface, these bubbles did not come into the liquid directly, but the bubbles moved along the heating surface and rose from the edge of

the surface. Namely, the bubbles on the lower surface stayed on the wall longer than those on the upper surface since the departure was governed mainly by the buoyant force.

Table 1 shows that the preparing period of the bubble generated on the lower surface is longer than that on the upper surface. This fact shows that longer staying period of bubbles might affect the destruction and disorder of the temperature field.

Table 1. One cycle of bubbling.

1. $q_0=7.75 \times 10^4 \text{ kcal m}^{-2}\text{h}^{-1}$, $T_0-T_s=9.2^\circ\text{C}$

(1) Bubbles generated on upper surface

(2) Bubbles generated on lower surface

	1 _a	1 _b	1 _c		1 _d	1 _e
t_p (s)	0.118	0.092	0.138	t_p (s)	0.249	0.236
t_g (s)	0.0239	0.0252	0.0246	t_g (s)	0.0438	0.0329
f (s ⁻¹)	7.05	8.55	6.14	f (s ⁻¹)	3.41	3.72
D_d (mm)	3.81	4.14	4.06	D_d (mm)	3.61	3.56
fD_d (mm s ⁻¹)	2.68	3.54	2.49	fD_d (mm s ⁻¹)	0.123	0.132
$t_g/(t_g+t_p)$	0.168	0.215	0.151	$t_g/(t_g+t_p)$	0.149	0.122

2. $q_0=1.62 \times 10^5 \text{ kcal m}^{-2}\text{h}^{-1}$, $T_0-T_s=14.0^\circ\text{C}$

(1) Bubbles generated on upper surface

(2) Bubbles generated on lower surface

	2 _a	2 _b	2 _c		2 _d	2 _e
t_p (s)	0.0219	0.0147	0.0485	t_p (s)	0.0692	0.0986
t_g (s)	0.0153	0.0184	0.0133	t_g (s)	0.0216	0.0247
f (s ⁻¹)	33.1	37.2	16.2	f (s ⁻¹)	10.9	8.12
D_d (mm)	2.54	3.00	2.15	D_d (mm)	3.19	2.88
fD_d (mm s ⁻¹)	8.41	11.1	3.48	fD_d (mm s ⁻¹)	3.47	2.34
$t_g/(t_g+t_p)$	0.505	0.687	0.216	$t_g/(t_g+t_p)$	0.235	0.201

3. $q_0=2.60 \times 10^5 \text{ kcal m}^{-2}\text{h}^{-1}$, $T_0-T_s=16.4^\circ\text{C}$

(1) Bubbles generated on upper surface

	3 _a	3 _b
t_p (s)	0.00207	0.00000
t_g (s)	0.01653	0.00878
f (s ⁻¹)	53.8	114
D_d (mm)	2.08	1.64
fD_d (mm s ⁻¹)	11.2	11.9
$t_g/(t_g+t_p)$	0.890	1.00

(2) Effect of heat flux. As shown in Fig. 4B, the bubble growth rate, the diameter of the bubbles departing from the wall and the growing period decrease as q_0 increases. The diameter of departing bubble, D_d , was defined as the equivalent diameter when the bubble height became maximum in any cases.

According to Zuber²⁾, when the heat flux q_0 is smaller than the following value

$$q_0 = \rho_v h_{fg} \frac{\pi}{6} 1.53 \left[\frac{\sigma g(\rho_l - \rho_v)}{\rho_l^2} \right]^{1/4} \frac{\text{Btu}}{\text{ft}^2 \text{h}} \quad (17)$$

D_d is constant and it is independent of q_0 : this region corresponds to the region of isolated bubble, in which the value of D_d can be approximated by the equation of Fritz³⁾, i.e.

$$D_{dF} = 0.021 \beta \left[\frac{\sigma}{g(\rho_l - \rho_v)} \right]^{1/2} \quad (18)$$

For the heat flux larger than the value calculated by equation (17), D_d is a function of q_0 : this region corresponds to the region of interference.

For water at atmospheric pressure, the heat flux given by equation (17) corresponds approximately to $1.4 \times 10^5 \text{ kcal m}^{-2} \text{h}^{-1}$ and D_{dF} corresponds to 2.63 mm from equation (18) with $\beta = 50^\circ$. (β ranged from 45° to 50° in the present experiments.)

Consequently, it is found that the boiling under $q_0 = 7.75 \times 10^4 \text{ kcal m}^{-2} \text{h}^{-1}$ is in the region of isolated bubbles in which there is yet much effect of non-boiling natural convection. The cases of $q_0 = 1.62 \times 10^5$ and $2.60 \times 10^5 \text{ kcal m}^{-2} \text{h}^{-1}$ are in the region of interference in which bubble motion promotes violently the destruction and disorder of the temperature field near the heating surface and the thermal layer thickness is reduced.

Now, the maximum thickness of thermal boundary layer on the lower surface of a horizontal plate in non-boiling natural convection corresponds approximately to 1.07 mm from Ref. 4. The thermal layer thickness in nucleate boiling is considered to be 0.5 mm for $q_0 = 7.75 \times 10^4 \text{ kcal m}^{-2} \text{h}^{-1}$ and 0.2 mm for $q_0 = 1.62 \times 10^5 \text{ kcal m}^{-2} \text{h}^{-1}$ respectively from Ref. 5 if we pay attention to the difference in boiling behaviour between two regions mentioned above. Hence, as the heat flux increases, a part of bubble within the thermal layer decreases after the bubble diameter has exceeded the thickness of thermal layer.

The base area of a bubble contacting with the wall increases with time until the bubble diameter parallel with the wall has become almost constant. Hereafter, the growth of bubble height from the surface becomes faster as compared with that of bubble diameter parallel with the wall, and the base

area decreases gradually until the bubble detaches from the wall.

From the fact mentioned above, it is assumed that a state in which the bubbles can depart from the wall is established when the bubble diameter parallel with the wall is almost constant in time and the base area has a maximum value. Thus, the buoyant force and the adhesive force due to surface tension in this state can be evaluated as follows:

For $q_0 = 7.75 \times 10^4 \text{ kcal m}^{-2}\text{h}^{-1}$

D_d (mm)	adhesive force due to surface tension (kg)	buoyant force (kg)
3.81	1.14×10^{-5}	1.73×10^{-5}
4.14	1.02×10^{-5}	2.02×10^{-5}
4.06	1.24×10^{-5}	2.21×10^{-5}

For $q_0 = 1.62 \times 10^5 \text{ kcal m}^{-2}\text{h}^{-1}$

2.54	5.22×10^{-6}	4.11×10^{-6}
3.00	8.25×10^{-6}	4.34×10^{-6}

This table shows that the ratio of the buoyant force to the adhesive force decreases as q_0 increases. It is also shown that the buoyant force is stronger than the adhesive force for $q_0 = 7.75 \times 10^4 \text{ kcal m}^{-2}\text{h}^{-1}$. However, the bubbles do not depart from the wall yet in that case calculated above. Hence, a force is acting on the bubble to push it against the wall. This force may be expressed by the left-hand side of Rayleigh's equation⁶⁾, i.e., equation

$$\rho_l \left[R \frac{d^2 R}{dt^2} + \frac{3}{2} \left(\frac{dR}{dt} \right)^2 \right] = p_v - p_0 - \frac{2\sigma}{R} \quad (19)$$

Namely, the repulsive force of the surrounding liquid against the bubble growth should be considered to be pushing the bubbles against the wall.

(3) Comparison with Zuber's and Griffith's theories. Forster and Zuber⁷⁾ and Plesset and Zwick⁸⁾ discussed detailed studies of the bubble growth problem in a uniformly superheated liquid by solving Rayleigh's equation and derived the following expression:

$$\rho_v h_{fg} \frac{dR}{dt} = b' \lambda \frac{T_0 - T_s}{\sqrt{\pi \alpha t}} \quad (20)$$

$$R = \frac{2b' \rho_l c}{\pi \rho_v h_{fg}} (T_0 - T_s) \sqrt{\pi \alpha t} \quad (21)$$

where the value of the constant, b' , was found to be $\sqrt{3}$ according to Plesset and Zwick's theory and $\pi/2$ to Forster and Zuber's. It was reported that these theories agreed well with Dergarabedian's data. However, it is improper that these theories for a uniformly superheated liquid apply to the growth of the

bubbles generated on the surface, since the temperature field is not uniform.

In developing the equation for bubble growth rate, Zuber⁹⁾ made a very interesting extension of these theories to cover the bubble growth rate for the case of a non-uniform temperature field. According to his theory, whereas only one heat transfer process occurs in a uniform temperature field, two transfers of energy take place in a non-uniform temperature field. One is the heat transfer across the thermal layer, this process maintains the evaporation at the bubble interface. The second is the heat transfer, q_b , from the vapour interface to the bulk liquid.

Consequently, Zuber considered the following energy balance instead of equation (20)

$$\rho_v h_{fg} \frac{dR}{dt} = b' \left[\lambda \frac{T_0 - T_s}{\sqrt{\pi \alpha t}} - q_b \right] \quad (22)$$

where q_b has time dependence because of the effect of turbulence due to bubble motion. Thus,

$$\rho_v h_{fg} \frac{dR}{dt} = b' \left[\lambda \frac{T_0 - T_s}{\sqrt{\pi \alpha t}} - c' t^n \right]$$

The value of the constant, c' , is determined from the condition that $dR/dt=0$ when $t=t_g$. It follows then that the relation between radius and time is given by

$$R = \frac{2b'}{\pi} \frac{\rho_l c}{\rho_v h_{fg}} (T_0 - T_s) \sqrt{\pi \alpha t} \frac{1}{2(n+1)} \left[2(n+1) - \left(\frac{t}{t_g} \right)^{n+1/2} \right] \quad (23)$$

$$R_d = \frac{2b'}{\pi} \frac{\rho_l c}{\rho_v h_{fg}} (T_0 - T_s) \sqrt{\pi \alpha t_g} \frac{2n+1}{2(n+1)} \quad (24)$$

$$\frac{D}{D_d} = \frac{R}{R_d} = \frac{1}{2n+1} \sqrt{\frac{t}{t_g}} \left[2(n+1) - \left(\frac{t}{t_g} \right)^{n+1/2} \right] \quad (25)$$

The results of Zuber's analysis are compared with the experimental results in Figs. 5 and 6. For the bubbles departing from upper surface, equation (25) with $n=1/2$ agrees with the experimental data for small t/t_g . However, equation (25) does not come to agree gradually as time increases, and the data of D/D_d increase rather straightly. Unfortunately, for the bubbles generated on the lower surface, it is so difficult to determine when the bubbles depart from the surface that the experimental data are scattering. However, generally speaking, the bubbles on the lower surface stay longer with almost constant diameter and therefore D/D_d is nearly equal to unity from $t/t_g \cong 0.5$.

Griffith¹⁰⁾ solved the same problem for growth of hemispherical bubble in subcooled liquid in the case of a linear variation of temperature with distance

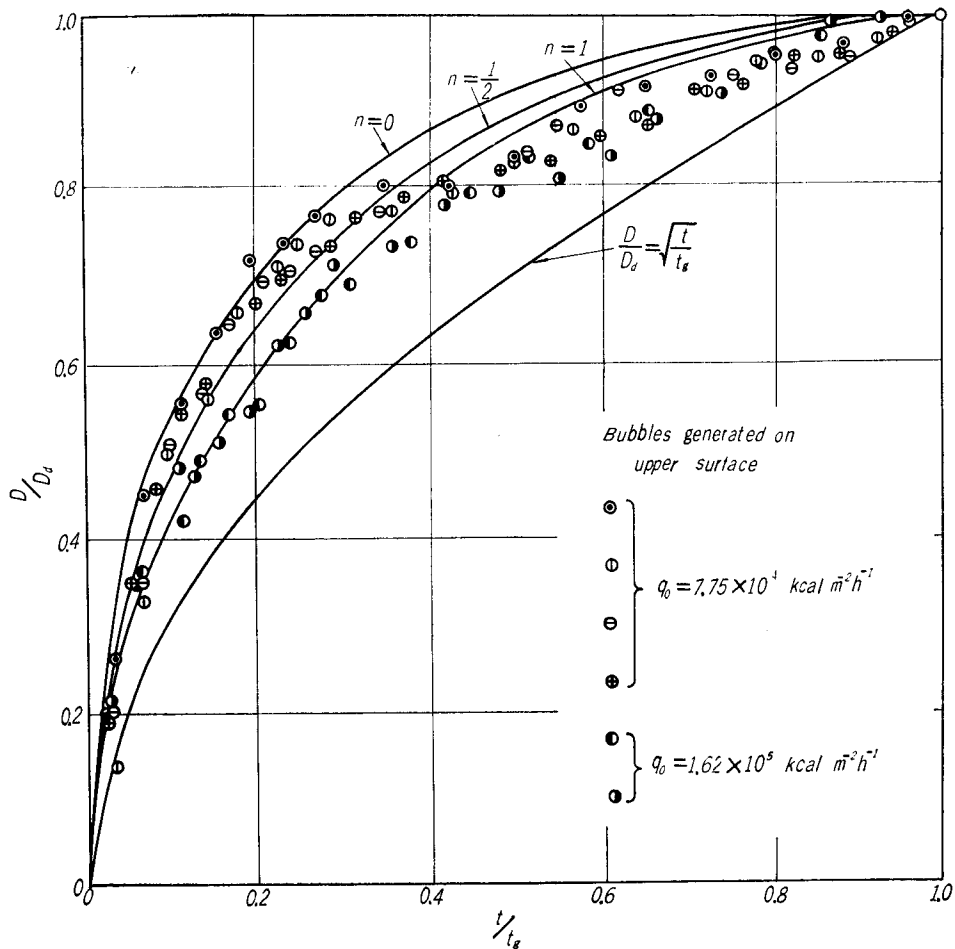


Fig. 5. Comparison of Zuber's equation (25) with experimental data.

from the surface to a certain distance b . Beyond b the liquid temperature was assumed uniform. His results, presented in a series of graphs, show the bubble growth for various conditions. The following parameter was of significance in correlating results: the ratio of superheat enthalpy per unit volume to latent heat enthalpy per unit volume,

$$c'' = \frac{\rho_l c (T_0 - T_s)}{\rho_v h_{fg}} \tag{26}$$

Fig. 7 illustrates the results of bubble growth by Griffith's analysis. In this case, the behaviour of bubble growth differs from the case of uniform temperature field, and the bubble does not grow with proportion to \sqrt{t} but it

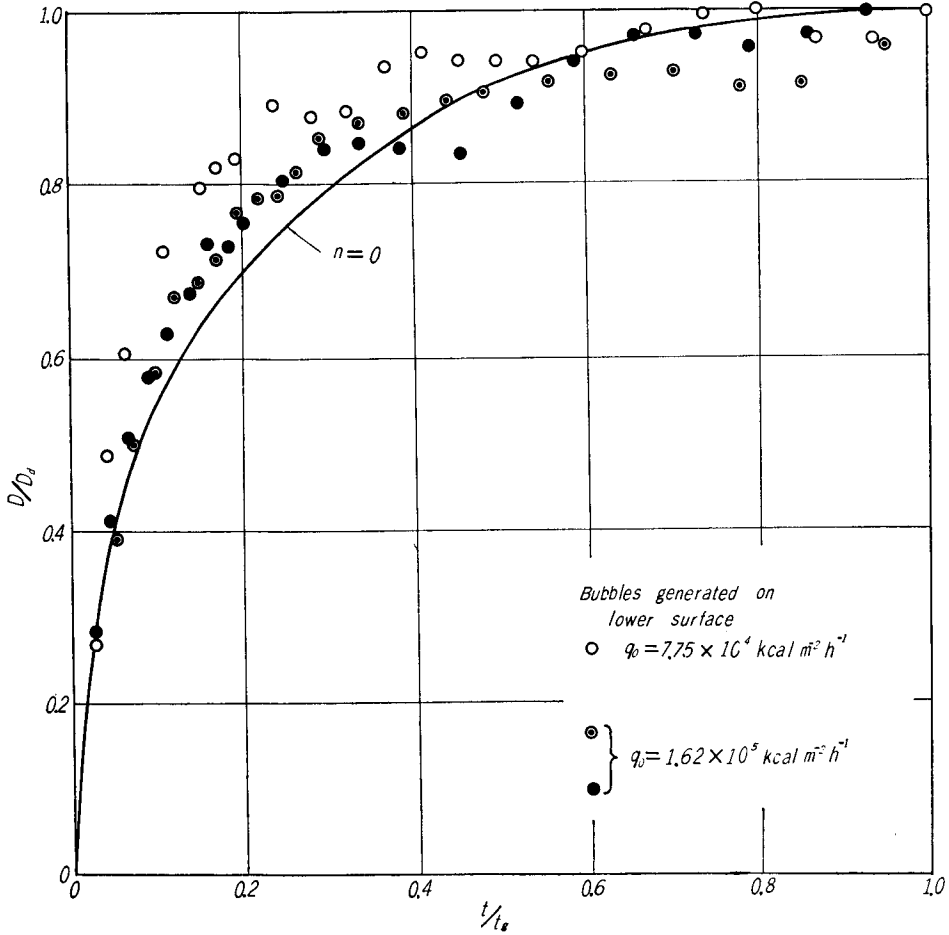


Fig. 6. Comparison of Zuber's equation (25) with experimental data.

grows more slowly after it has become a certain size.

Fig. 8 shows the experimental results. The parameter c'' was obtained as 28.4 for $q_0 = 7.75 \times 10^4 \text{ kcal m}^{-2} \text{ h}^{-1}$ and 43.2 for $q_0 = 1.62 \times 10^5 \text{ kcal m}^{-2} \text{ h}^{-1}$ by using equation (26). Griffith made mention neither the cases in which c'' was larger than 10.6 nor the way to determine the thermal layer thickness b . However, as described in the above section (2), b is assumed to be 0.5 mm for $q_0 = 7.75 \times 10^4 \text{ kcal m}^{-2} \text{ h}^{-1}$ and 0.2 mm for $q_0 = 1.62 \times 10^5 \text{ kcal m}^{-2} \text{ h}^{-1}$ respectively. In Fig. 8, τ and Y were thus obtained by using these values of the thermal layer thickness. As compared with Fig. 7, it is found that there is a similar tendency in relation to the effects of parameter c'' .

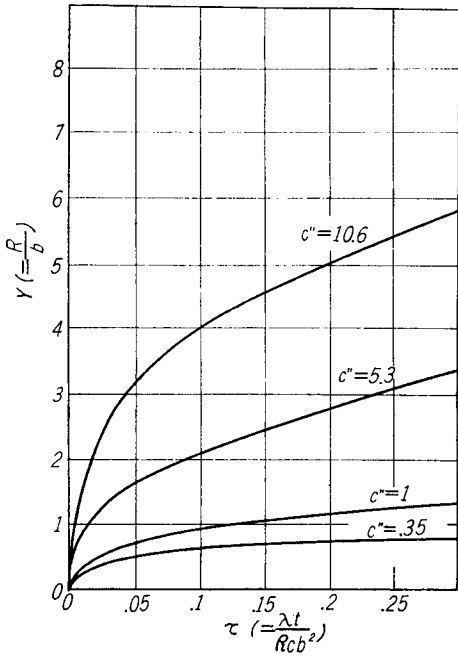


Fig. 7. Calculated bubble growth rates for saturated bulk temperature $T_s = T_l$. [Griffith, 10)]

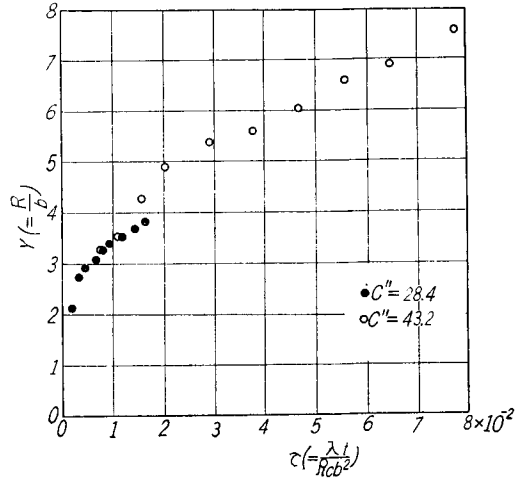


Fig. 8. Y vs. τ .

5. Some Discussions on Diameter of Detached Bubble and Frequency of Bubbling

The experimental data of preparing period, t_p , growing period, t_g , frequency of bubble formation, f , and bubble diameter when the bubble detaches from the heating surface, D_d , are tabulated in Table 1. As shown in this table, both the preparing period and the growing period of bubbles coming from the lower surface are longer than those from the upper surface. Namely, the values of frequency of bubble formation on the upper surface are larger than those on the lower surface. However, there is not much difference in the diameters of the departing bubbles at given heat flux.

Fig. 9 illustrates the relationship between D_d and q_0 , and it shows that D_d decreases exponentially as q_0 increases.

Now, based on bubble rise-velocities, Zuber

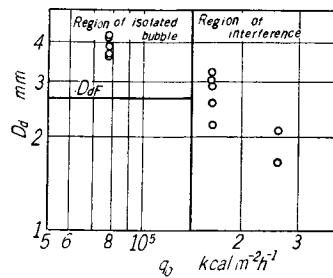


Fig. 9. Variation of bubble diameter at departure with heat flux.

proposed the following relation¹¹⁾,

$$fD_d = 1.18 \frac{t_g}{t_g + t_p} \left[\frac{\sigma g(\rho_l - \rho_v)}{\rho_l^2} \right]^{1/4} \quad (27)$$

where the value of constant, 1.18, was obtained from experiments by many investigators. From the definition of frequency of bubbling, f is given by

$$f = \frac{1}{t_g + t_p}$$

Thus, the diameter of a departing bubble is shown as follows :

$$D_d = 1.18 t_g \left[\frac{\sigma g(\rho_l - \rho_v)}{\rho_l^2} \right]^{1/4} \quad (28)$$

Equation (28) means that the relationship between D_d and t_g is a linear equation. This relationship is shown in Fig. 10. From this figure, it was found that in order to obtain an agreement with the present experimental data, it was necessary to take the value of 1.08 for the constant in equation (28) instead of 1.18, namely,

$$fD_d = 1.08 \frac{t_g}{t_g + t_p} \left[\frac{\sigma g(\rho_l - \rho_v)}{\rho_l^2} \right]^{1/4} \quad (29)$$

Jakob¹²⁾ found that $t_g/(t_g + t_p)$ was nearly constant and $t_g \cong t_p$. In this case, equation (27) becomes

$$fD_d = \frac{1.18}{2} \left[\frac{\sigma g(\rho_l - \rho_v)}{\rho_l^2} \right]^{1/4} \quad (30)$$

Jakob reported that this equation agreed well with the experimental data. However, since Table 1 and Fig. 10 show that t_g is not considered to be equal to t_p and D_d is considered to be a function of t_g , it seems improper to conclude that fD_d is constant.

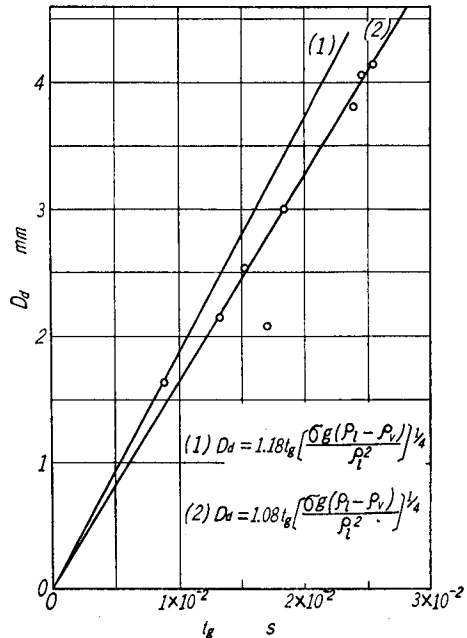


Fig. 10. Variation of bubble diameter at departure with growing period.

6. Conclusion

In conclusion, the experimental evidence deduced from these findings can be summarized as follows :

- (1) Both the preparing period and the growing period of bubbles which occur on the lower surface were longer than those on the upper surface.

(2) The values of the preparing period, the growing period and the diameter of departing bubbles decreased as the heat flux q_0 increased. The equivalent diameter of bubble increased more slowly with time as the heat flux increased.

(3) With consideration for a decrease in the thermal layer thickness as boiling became intensive, it was found that Griffith's theory showed the same tendency as the experimental results. Zuber's equation (25) agreed well with the experimental data for small t/t_g .

(4) While the bubbles are growing, there is a force pushing them against the wall: this is considered to be a repulsive force of the surrounding liquid against the bubble growth.

(5) It is said in general that the product of D_d and f is constant. However, the present experimental results indicate that D_d is a linear function of t_g . Thus, fD_d is considered not to be constant but to be a function of t_g and t_p as shown by equation (29).

Acknowledgement

The authors wish to thank Messrs. K. Uematsu and H. Kashiwara for their discussions and their experimental works.

Nomenclature

- b : thickness of thermal layer
- b' : constant
- c : specific heat of liquid
- c' : constant
- c'' : parameter defined by equation (26)
- D : bubble diameter, defined as the diameter of sphere equivalent to the volume of actual bubble.
- D_d : diameter of departing bubble
- D_{dF} : diameter of departing bubble predicted by Fritz³⁾
- E : heat energy, defined by equation (12) or (13)
- f : frequency of bubble formation
- g : acceleration due to gravity
- h_{fg} : latent heat of evaporation
- k : Boltzmann constant
- n : exponent of t
- p : pressure
- p_0 : pressure of bulk liquid

- p_v : pressure of vapour inside bubble
 q : heat flux
 q_b : heat flux from vapour interface to bulk liquid
 q_0 : heat flux in steady state
 R : bubble radius
 R_d : radius of departing bubble
 r^* : critical radius of embryonic bubble
 t : time
 t_g : growing period
 t_p : preparing period
 T : temperature
 T_i : initial temperature
 T_l : bulk liquid temperature
 T_0 : surface temperature of heated wall in steady state corresponding to q_0
 T_s : saturation temperature of liquid at p_0
 T_w : surface temperature of heated wall
 x : distance from the surface, normal to the wall
 Y : dimensionless bubble radius $Y=R/b$
 α : thermal diffusivity
 β : contact angle of bubble
 λ : thermal conductivity of liquid
 A : latent heat of evaporation referred to one molecule
 ρ_l : density of liquid
 ρ_v : density of vapour
 σ : surface tension
 τ : dimensionless time $\tau=\lambda t/\rho_l c b^2$

References

- 1) I. Michiyoshi, K. Uematsu & T. Nakajima, *Memoirs of the Faculty of Engng. Kyoto University* **26** (1964), 16.
- 2) N. Zuber, *Intern. J. Heat Mass Transfer* **6** (1963), 53.
- 3) W. Fritz, *Phys. Z.* **36** (1935), 379.
- 4) S. Sugawara & I. Michiyoshi, *Trans. Japan Soc. Mech. Engrs.* **21** (1955), 109.
- 5) M. Akiyama, *Studies of Boiling Heat Transfer*, Japan Soc. Mech. Engrs. (1963).
- 6) L. Rayleigh, *Phil. Mag.* **34** (1917), 94.
- 7) H. K. Forster & N. Zuber, *J. Appl. Phys.* **25** (1954), 474.
- 8) M. S. Plesset & S. A. Zwick, *J. Appl. Phys.* **25** (1954), 493.
- 9) N. Zuber, *Intern. J. Heat Mass Transfer* **2** (1961), 83.
- 10) P. Griffith, *Trans. Am. Soc. Mech. Engrs.* **80** (1958), 721.
- 11) W. Ibel, *Modern Developments in Heat Transfer* 114 (1963), Academic Press, N. Y. and L.
- 12) M. Jakob, *Heat Transfer I*, 2nd ed. 633 (1954), John Wiley & Sons, Inc., N. Y.